Journal of Industrial Information Technology and Application *ISSN(Online): 2586-0852*
Vol.7 No.4

Effect Analysis of 3D Printed Radome on Performance of 24 GHz RADAR Antenna

Junho Yeo[1*)]
[1)] School of Artificial Intelligence, Daegu University, Korea.

Abstract. In this paper, the effects of placing a 3D printed radome on the performance of a 24 GHz RADAR antenna are analyzed. First, a 4 by 1 linear microstrip patch array antenna operating in the frequency range of 24.0 – 24.25 GHz with a shunt connected series feed network is designed on a HF-350F substrate (ε_r = 3.5, h = 0.254 mm, tan δ = 0.0029), as a reference RADAR antenna. Next, the 4 by 1 patch array antenna is placed inside a hollow hemi-sphere radome with a thickness of 3.724 mm. Polylactic acid (PLA), which is a commonly used material for fused deposition modeling (FDM) – type 3D printers, is chosen for the radome material. The effects of varying the radius of the hemi-sphere PLA radome on the input reflection coefficient, radiation patterns, and gain of the 4 by 1 patch array antenna are investigated. In this work, the distance between the array antenna and the hemi-sphere radome is the inner radius of the hemi-sphere radome.

Keywords. radome; radio detection and ranging (RADAR); patch array antenna; 3D printer; polylactic acid (PLA)

1. Introduction

A radome is a portmanteau of radar and dome, and it is a cover or enclosure to protect a radar system or antenna from environmental influences, such as rain, snow, wind, dust, and temperature [1]. Theoretically, the radome should be transparent to the received and transmitted electromagnetic waves without any degradation of the antenna performance. The simplest radome is a single-layer structure with a homogeneous half-wavelength thick dielectric material. The shape of the radome can be planar, spherical, or hexahedron. Typically used radome material are low loss dielectric materials, such as polybutylene terephthalate (PBT), plexiglass, polycarbonate, polytetrafluoroethylene, polystyrene, and acrylonitrile butadiene styrene (ABS) [2].

* Corresponding author: jyeo@daegu.ac.kr
Received: Apr 20, 2023; Accepted: May 29, 2023; Published: Dec 31, 2023

Since World War II, various radar systems have been used for military and commercial applications. Recently, millimeter-wave radars have been widely applied in advanced driver assistance system (ADAS) and automated driving system (ADS) of high-performance or autonomous cars, because of their advantages compared to cameras, LiDARs, and ultrasonic sensors, such as high range, operability in any weather condition, and velocity resolution [3]. Millimeter wave is defined as the frequency band with the wavelength between 10 millimeters (30 GHz) and 1 millimeters (300 GHz) in the air. The current frequency bands of the automotive millimeter wave radar are divided into three types: 24 GHz, 77 GHz, and 79 GHz [4]. The 24 GHz millimeter wave radar with short sensing range from 0.15 meters to about 30 meters is mainly used as a parking assistance. The 77 GHz radar with medium sensing range from 1 meter to about 100 meters is used for blind spot detection. The 79 GHz radar with long sensing range up to 250 meters is used in adaptive cruise control and the forward collision warning system to provide the driver with sufficient response time for braking or dodging. Recently, the 60 GHz radar is used to detect the driver's hand gestures to control the car interface and detect the number and type of passengers to provide safety assistance.

The types of antennas used for radar systems can be classified as reflector antennas, lens antennas, and array antennas [5]. For commercial millimeter wave radars, a variety of planar microstrip patch array antennas have been mainly used. For the feed network of the microstrip patch array antennas for the commercial millimeter wave radars, in line and shunt connected series feed networks have been widely used.

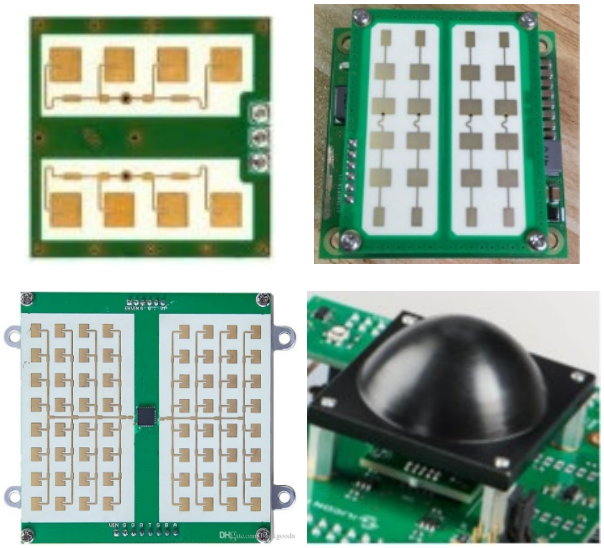

Figure 1. Examples of 24 GHz commercial radar antennas.

In this paper, the performance of a 24 GHz RADAR antenna when the antenna is placed inside a 3D printed radome is investigated. A 4 by 1 linear microstrip patch array antenna with a shunt connected series feed network is designed and used as a reference antenna. A hemi-spherical hollow radome made of polylactic acid (PLA) using a 3D printer is designed. The input reflection coefficient, radiation patterns, and gain of the 4 by 1 microstrip patch antenna inside the radome when the radius of the radome varies are studied.

2. 4 by 1 Linear Array with Shunt Connected Series Feed Network and Tapered Amplitude Distribution

A 4 by 1 linear square microstrip patch array antenna with a shunt connected series feed network and a tapered amplitude distribution is designed, as shown in Fig. 1(a).

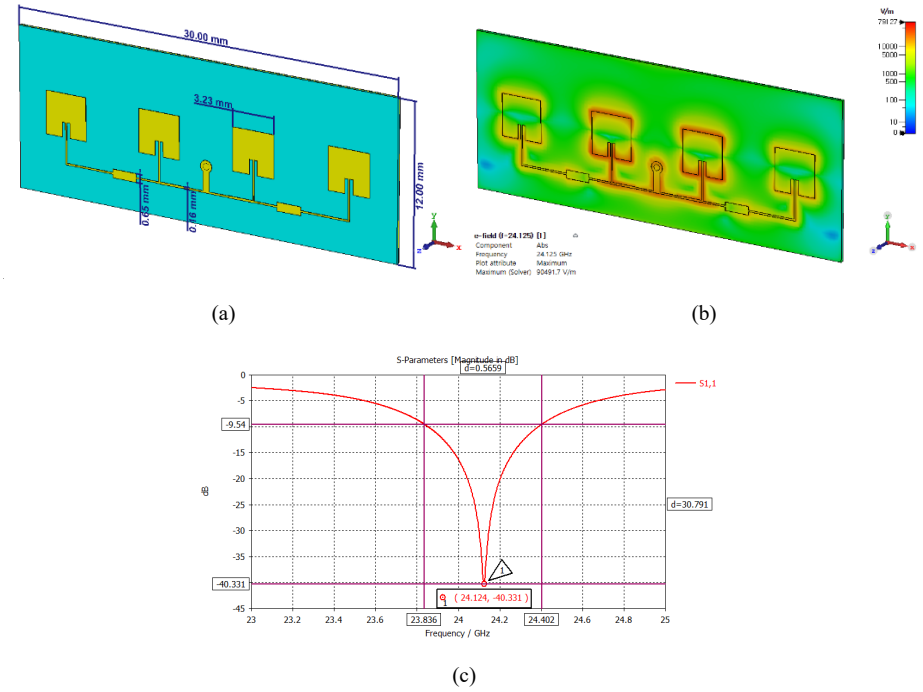

Figure 2. (a) Geometry, (b) electric field distribution at 24.125 GHz, and (c) S_{11} characterisitc of 4 by 1 microstrip patch antenna with tapered amplitude distribution.

The spacing between the array elements is chosen to be 7.494 mm, which is about one guided wavelength at 24.125 GHz, and the length of the square patch is designed to 3.23 mm. A shunt connected series feed network is designed to provide a tapered amplitude with 1:5:5:1 power ratio to decrease sidelobe levels, as shown in Fig. 1(b).

The width and length of the ground plane are 30 mm and 12 mm, respectively. The simulated frequency bandwidth for a VSWR less than 2 is 23.836 – 24.402 GHz.

Simulated realized gain at z-axis direction as a function of frequency and radiation patterns at 24.125 GHz are plotted in Fig. 5. Peak gain at 24.125 GHz is 11.11 dBi. Half power beam width for z-x plane, which is along the 4 by 1 array axis, is 26.6 degrees with sidelobe level of -13.9 dB, whereas that for y-z plane is 75.5 degrees.

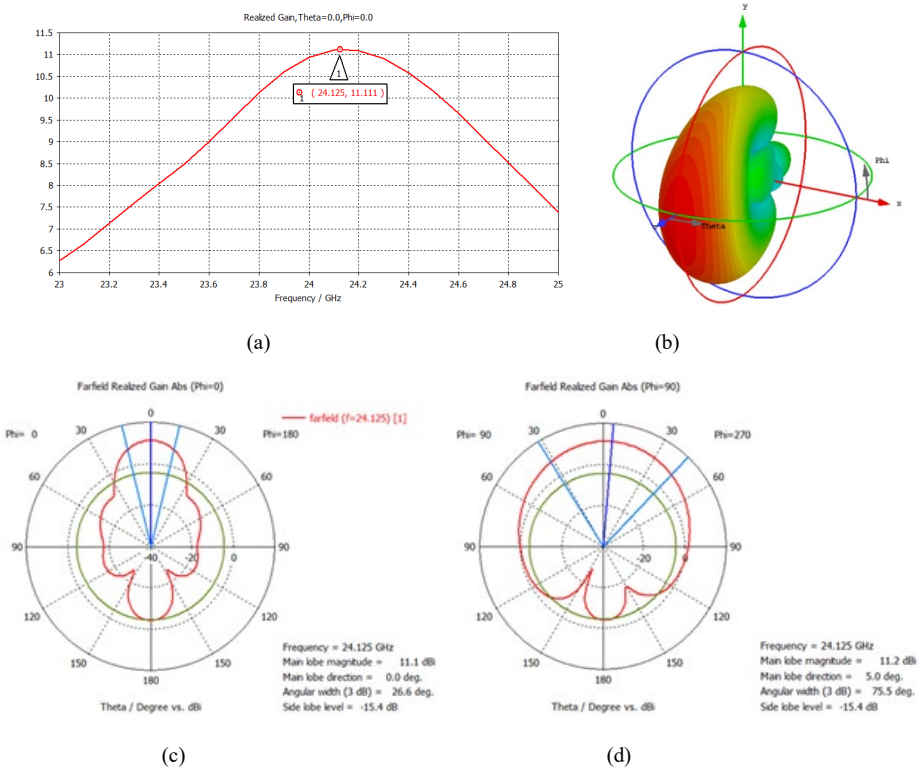

Figure 3. (a) realized gain at z-axis direction, (b) 3D radiation pattern at 24.125 GHz, (c) radiation pattern for *z-x* plane at 24.125 GHz, (d) radiation pattern for *y-z* plane at 24.125 GHz.

3. Effect of 3D Printed Radome on 4 by 1 Linear Array Antenna

3D (three dimensional) printing is an inexpensive and easy method to realize any arbitrary geometry of electronic or radio frequency (RF) component prototypes [6]. Among various 3D printing methods with layer-by-layer manufacturing processes, such as stereolithography (SLA), fused deposition modeling (FDM), and digital light processing (DLP), FDM is the most mature and popular method, and filaments are heated and extruded from the printer head and deposited onto the print bed in a shape

defined by the computer aided design (CAD) file in a continuous flow [7]. Polylactic acid (PLA), which is a commonly used material for FDM – type 3D printers, is chosen for the radome material. The relative permittivity (ε_r) and loss tangent (tan δ) of PLA near 24 GHz band are 2.788 and 0.054, respectively [8].

In order for the radome to become nearly transparent, the minimum thickness of the radome is the half of the wavelength in radome material, as expressed in the following equation [9]:

$$T_m = \frac{\lambda_m}{2} = \frac{\lambda_0}{2\sqrt{\varepsilon_r}} \tag{1}$$

$$\lambda_0 = \frac{c}{f_0} \tag{2}$$

where T_m is the radome thickness, λ_m is the wavelength in radome material, λ_0 is the wavelength in freespace, ε_r is the relative permittivity of radome material, c is the speed of light in freespace, and f_0 is the center operating frequency of RADAR

The distance between the antenna and the radome can be an integer multiple of the half of the freespace wavelength:

$$d_m = \frac{n \cdot \lambda_0}{2} \tag{3}$$

where d_m is the distance between the antenna and the radome and n is the integer

For ε_r = 2.788 and f_0 = 24.125 GHz, the minimum thickness of the PLA radome is T_m = 3.724 mm, and the minimum distance between the antenna and the PLA radome is $d_{m,1}$ = 6.2 mm. Since the longest dimension of the 4 by 1 linear microstrip patch antenna designed in the previous section is 30 mm and the distance between the antenna and the radome d_m becomes the inner radius of the hemi-sphere when the 4 by 1 array antenna is placed in the origin of the hollow hemi-sphere radome, the minimum possible integer in (3) is 3 and the distance for this case is $d_{m,3}$ = 18.6 mm. Fig. 4 shows the geometry of the 3.724 mm-thick hemi-sphere radome with the 4 by 1 array antenna placed inside.

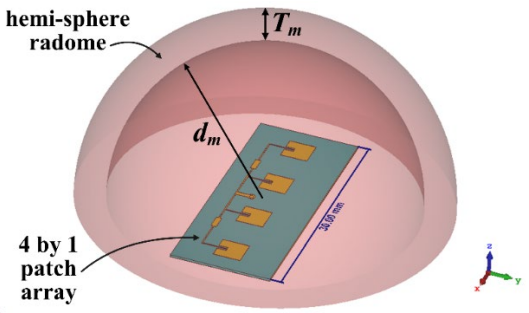

Figure 4. Geometry of hemi-sphere radome with 4 by 1 array antenna placed inside.

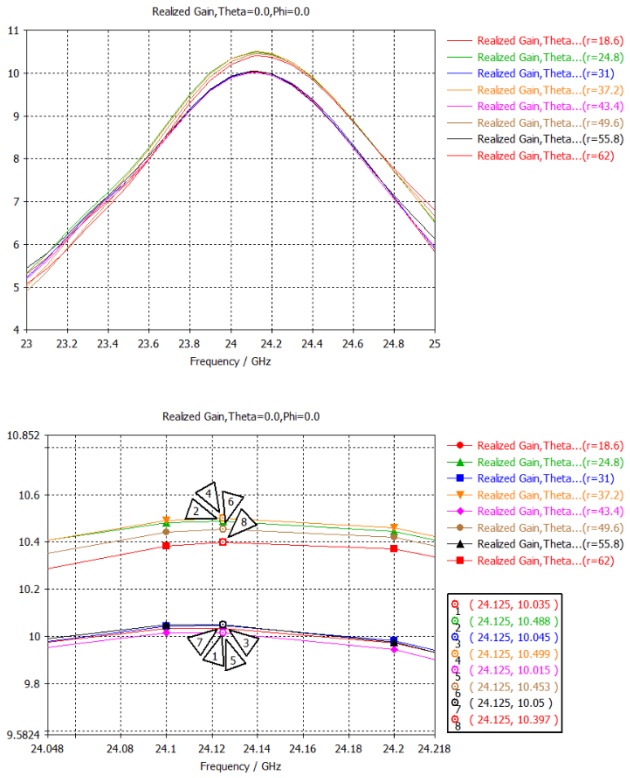

Figure 5. Realized gain characteristics of the 4 by 1 array antenna with the hemi-sphere radome for boresight direction (+z direction) at 24.125 GHz when the distance varies from 18.6 mm to 62 mm.

Next, the effects of varying the distance between the array antenna and the hemi-sphere radome on the radiation patterns and realized gain characterisitcs of the array antenna are investigated. In this case, the distance between the array antenna and the hemi-sphere radome is the same as the inner radius of the hemi-sphere radome when the array antenna is placed the origin of the hemi-sphere. The distance values used for the simulation are d_m = 18.6 mm, 24.8 mm, 31 mm, 37.2 mm, 43.4 mm, 49.6 mm, 55.8 mm, and 62 mm corresponding to the integer n = 3, 4, 5, 6, 7, 8, 9, and 10 in (3). Realized gain characteristics for boresight direction (+z direction) when the distance varies from 18.6 mm to 62 mm with a step of 6.2 mm are presented in Fig. 5. We can see from Fig. 5 that there exists some reduction in realized gain characteristics due to the loss tangent of the radome material and they are divided into two groups according to peak gain value at 24.125 GHz. The first group is when the integer of (3) is an even number and peak gain at 24.125 GHz is 10.397 ~ 10.499 dBi, whereas the second group is when the integer is an odd number and peak gain at 24.125 GHz is 10.015 ~ 10.05 dBi. Peak gain of the first group is 0.382 ~ 0.449 dB larger than that of the second group. In addition, peak

gain of the first group decreases 0.612 ~ 0.714 dB compared to the case without the radome in Fig.3, whereas it decreases 1.061 ~ 1.096 dB for the second group. Therefore, peak gain value at 24.125 GHz is the largest when the integer is 6, that is, d_m = 6×6.2 mm = 37.2 mm.

Figs. 6 and 7 show the radiation patterns on the *y-z* (Phi = 90°) and *z-x* (Phi = 0°) planes. There exist ripples in the radiation patterns because of the multiple reflections at the radome interface boundary. For the first group, the ripple is maximum at boresight (+z) direction, whereas it is minimum for the second group and this causes more decrease in peak gain.

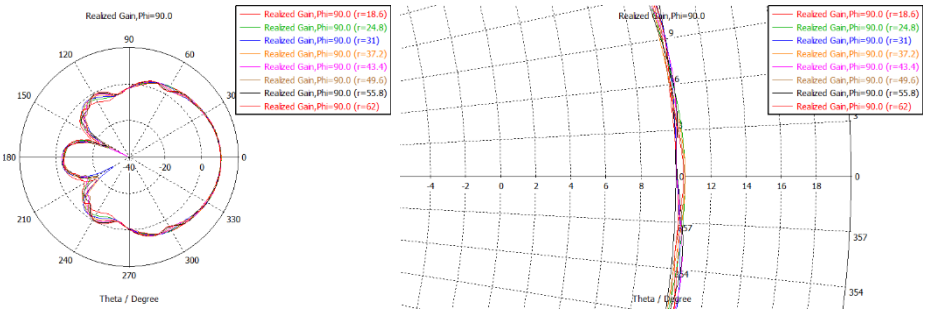

Figure 6. Radiation patterns on the *y-z* (Phi = 90°) plane at 24.125 GHz for varying the distance from 18.6 mm to 62 mm.

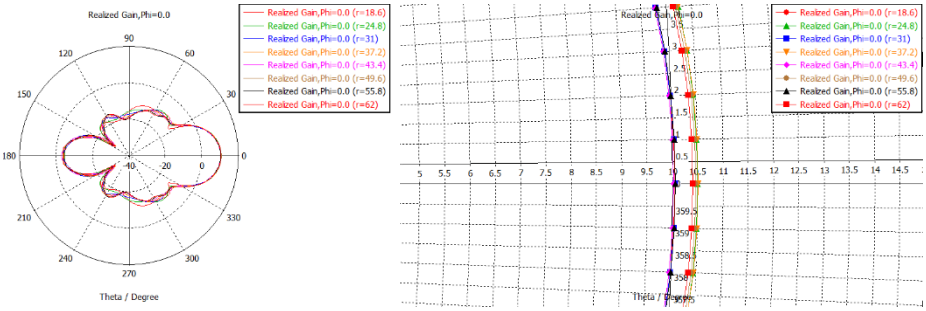

Figure 7. Radiation patterns on the *z-x* (Phi = 0°) plane at 24.125 GHz for varying the distance from 18.6 mm to 62 mm.

The radiation patterns of the 4 by 1 array antenna with the radome for d_m = 37.2 mm are shown in Fig. 8.

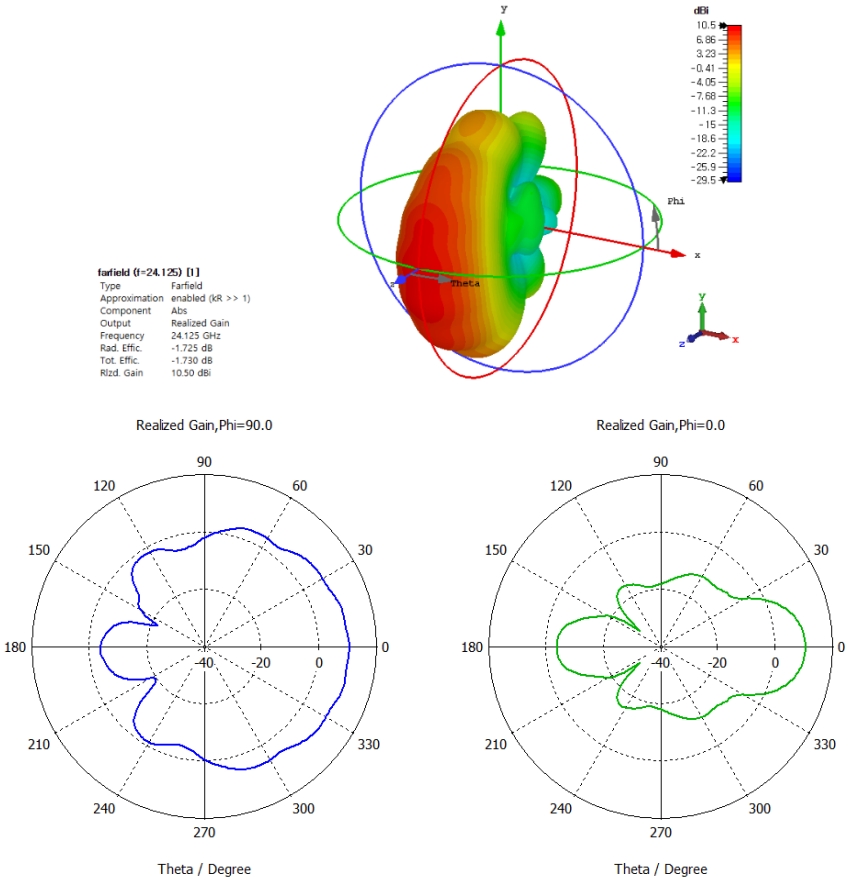

Figure 8. Radiation patterns of the 4 by 1 array antenna with the radome for d_m = 37.2 mm.

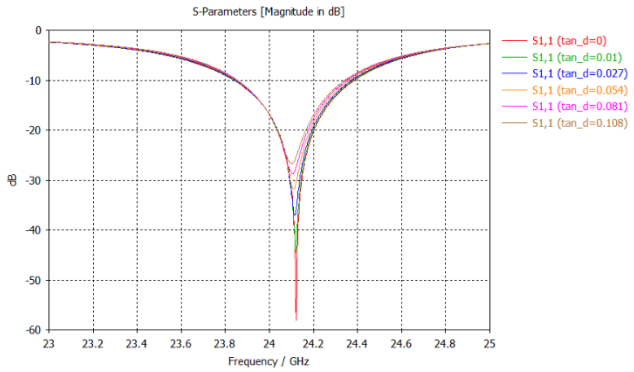

(a)

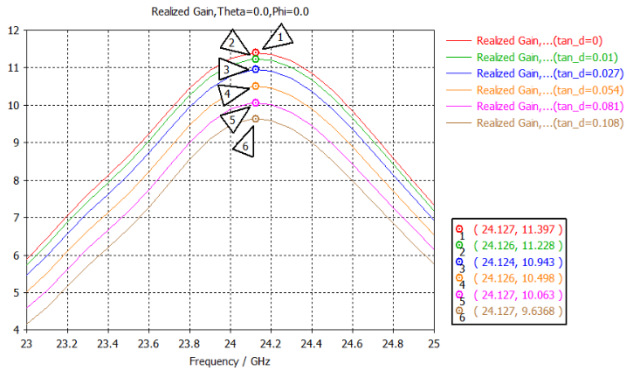

(b)

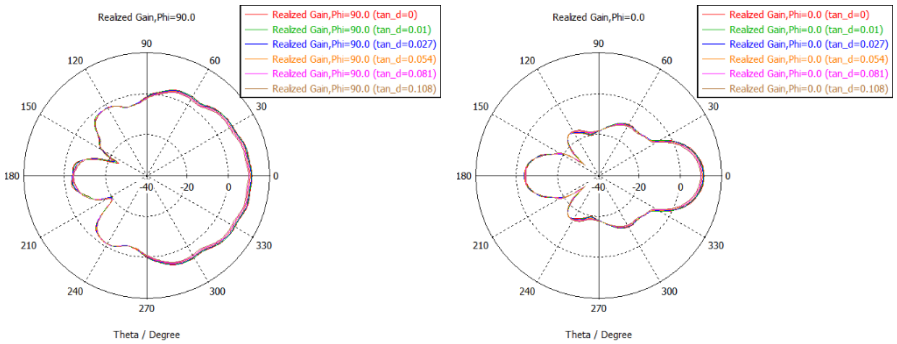

(c) (d)

Figure 9. (a) input reflection coefficient, (b) realized gain at z-axis direction, (c) radiation pattern for *y*-*z* plane at 24.125 GHz, (d) radiation pattern for *z*-*x* plane at 24.125 GHz.

Finally, the effects of varying loss tangent of the PLA radome material on the antenna performance for d_m = 37.2 mm are studied. Loss tangent varies from 0 to 0.108. We can see that the level of the input reflection coefficient increases as loss tangent increases due to the increased dielectric loss. Accordingly, Peak gain at 24.125 GHz decreases from 11.397 dB to 9.637 dB as loss tangent increases from 0 to 0.108.

4. Conclusion

We have studied the radiation patterns and gain characteristics of a 4 by 1 microstrip patch array antenna with a 3D printed PLA hemi-sphere radome for 24 GHz RADAR applications, when the distance between the radome and the array antenna placed inside the radome varies. The distance between the array antenna and the radome is the same as the inner radius of the hemi-sphere radome when the array antenna is placed the origin

of the hemi-sphere. Since the distance can be an integer multiple of the half of the freespace wavelength and the longest dimension of the array antenna is 30 mm, the distance (d_m) values of 18.6 mm, 24.8 mm, 31 mm, 37.2 mm, 43.4 mm, 49.6 mm, 55.8 mm, and 62 mm are used, which corresponds to the integer n = 3, 4, 5, 6, 7, 8, 9, and 10.

It was found that there exist ripples in the radiation patterns because of the multiple reflections at the radome interface boundary, and the multiple reflections and the loss tangent of the radome material cause the reduction in realized gain characteristics. In addition, the results can be divided into two group according to the peak gain at 24.125 GHz. The first group is when the integer is an even number, whereas the second group is when the integer is an odd number. Peak gain of the first group is 0.382 ~ 0.449 dB larger than that of the second group. Peak gain of the first group decreases 0.612 ~ 0.714 dB compared to the case without the radome, whereas it decreases 1.061 ~ 1.096 dB for the second group. Peak gain value at 24.125 GHz is the largest when the integer is 6 with the distance d_m = 6×6.2 mm = 37.2 mm, which means the lowest reduction in realized gain. Therefore, we can choose the distance between the array antenna and the radome as 37.2 mm.

References

[1] Z. Qamar, J. L. Salazar-Cerreno, and N. Aboserwal, “An ultra-wide band radome for high-performance and dual-polarized radar and communication systems,” IEEE Access, vol. 8, pp. 199369-199381, 2020

[2] C. Kumar, H. U. R. Mohammed, and G. Peake, “Mmwave radar radome design guide,” application report, Texas Instruments, Aug. 2021.

[3] M. M. S. Hossain, S. A. N. Saqueb, A. H. Arage, J. Cabigao, C. Velasquez, and N. K. Nahar, “Wideband Radomes for Millimeter-Wave Automotive Radars,” IEEE Transactions on Antennas and Propagation, vol. 70, no. 2, pp. 1178-1186, Feb. 2022

[4] https://www.allion.com/automotive/incar-mmwave-radar/

[5] B. Edde, Radar: Principles, Technology, Applications, Englewood Cliffs, NJ: Prentice Hall, 1992.

[6] G. S. Karthikeya, S. K. Koul, A. K. Poddar, and U. Rohde, “Path loss compensated millimeter wave antenna module integrated with 3D-printed radome,” International Journal of RF and Microwave Computer-Aided Engineering, vol. 30, e22347, 2020.

[7] E. S. Rosker, R. Sandhu, J. Hester, M. S. Goorsky, and J. Tice, “Printable materials for the realization of high performance RF components: challenges and opportunities,” International Journal of Antennas and Propagation, vol. 2018, Article ID 9359528, pp. 1-19, 2018.

[8] D. Yoon, J. H. Kim, N. Yoon, K. H. Oh, D. W. Woo, and Y. B. Park, “Time-gated free-space measurement signal processing method to estimate dielectric constant of 3D printed materials,” J. Korean Inst. Electromagn. Eng. Sci., vol. 33, no. 6, pp. 498-508, Jun. 2022.

[9] RFbeam Microwave GmbH: Radome (Radar enclosure), Application Note AN03, 2013. <http://www.rfbeam.ch/fileadmin/downloads/appnotes/AN-03-Radome.pdf>